2005 International Symposium on Nonlinear
Theory and its Applications (NOLTA2005)
Bruges, Belgium, October 18-21, 2005

A Numerical Analysis on Stability of Simplest Passive Dynamic Walking

Masayuki Baba† and Takashi Hikihara†

†Department of Electrical Engineering, Kyoto University
Katsura, Nishikyo, Kyoto, 615-8510 JAPAN
Email: baba@dove.kuee.kyoto-u.ac.jp, hikihara@kuee.kyoto-u.ac.jp

Abstract—This paper focuses on the stability of passive dynamic walking. Passive dynamic walking is well known as efficient and natural walking, so that many researchers investigate the mechanism to apply it to the locomotion with natural and effective energy use. The investigation of the stability on this motion has a potential to lead us to design more efficient or natural control. In this paper, the stability of the simplest passive dynamic walking is mainly discussed based on the global phase structure, considering the continuous walking state. As a result, the dynamical feature of passive dynamic walking is clearly understood.

1. Introduction

This paper addresses the stability of passive dynamic walking. Passive dynamic walking [1] is a mechanism, through which the biped robot walks down an inclined plane without active control. Then the energy for walking is fed by the conversion of gravitational potential energy. The motion of passive dynamic walking is only governed by the dynamics of itself, autonomously.

The passive dynamic walking is efficient walking and has a steady gait [2, 3, 4]. Several biped robots that use the passive dynamic walking with active torque input are developed [5, 6], and they actually achieve the locomotion under less energy use even on the level ground. The stability of compass gait is also discussed [3, 7, 8]. However, most of the discussions are based on the linearized local stability and the global dynamics has not been still confirmed. The detection of the global behavior of passive dynamic walking leads us to realize more efficient or natural walking. This paper numerically addresses the outline about the global stability of passive dynamic walking related to global stability.

2. Compass gait model

Figure 1 shows a simple 2-D model of a biped robot. The biped robot does not have any actuator and any controller. Each leg is knee-less and rigid structure, and is equivalent to the other leg and is linked with the hip by a frictionless joint. The leg touching the ground is called *stance leg*, and the other leg which can freely swing, *swing leg*. The nomenclature of symbols in the figure is presented in Tab. 1. During the swing of legs, the toe of stance leg is assumed to be fixed. Thus the dynamic equation of the biped robot

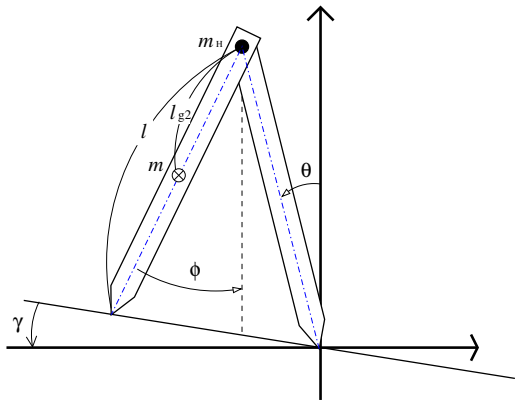

Figure 1: A simple biped robot model.

is obtained:

$$\begin{cases} \dfrac{\mathrm{d}\theta}{\mathrm{d}t} = \dot{\theta}, \\ \dfrac{\mathrm{d}\phi}{\mathrm{d}t} = \dot{\phi}, \\ \dfrac{\mathrm{d}\dot{\theta}}{\mathrm{d}t} = \dfrac{-M_{11}\dot{\theta}^2 + M_{12}\dot{\phi}^2 + G_1}{I_1(ml_{g2}^2 + I) - \{mll_{g2}\cos(\theta-\phi)\}^2}, \\ \dfrac{\mathrm{d}\dot{\phi}}{\mathrm{d}t} = \dfrac{-M_{21}\dot{\theta}^2 + M_{22}\dot{\phi}^2 + G_2}{I_1(ml_{g2}^2 + I) - \{mll_{g2}\cos(\theta-\phi)\}^2}, \end{cases} \tag{1}$$

where

$$\begin{cases} I_1 = m_H l^2 + m(l-l_{g2})^2 + ml^2 + I, \\ M_{11} = m^2 l^2 {l_{g2}}^2 \cos(\theta-\phi)\sin(\theta-\phi), \\ M_{12} = mll_{g2}(I + ml_{g2}^2)\sin(\theta-\phi), \\ M_{21} = I_1 mll_{g2}\sin(\theta-\phi), \\ M_{22} = m^2 l^2 {l_{g2}}^2 \cos(\theta-\phi)\sin(\theta-\phi), \\ G_1 = \{(m_H+2m)l - ml_{g2}\}(I+ml_{g2}^2)g\sin\theta \\ \qquad -m^2 l{l_{g2}}^2 g\cos(\theta-\phi)\sin\phi, \\ G_2 = \{(m_H+2m)l - ml_{g2}\}mll_{g2}g\cos(\theta-\phi)\sin\theta \\ \qquad -I_1 mll_{g2}g\sin\phi. \end{cases}$$

These equations correspond to those for the double pendulum. There exists no energy loss during the swing of legs, so that the whole energy is conserved during the swing motion. When the swing leg touches the ground, a transition between legs occurs at the end of the step, and the stance leg simultaneously leaves the ground to take the next step.

Table 1: Nomenclature.

θ	Angle of stance leg with vertical
ϕ	Angle of swing leg with vertical
$\dot{\theta}$	Angular velocity of stance leg
$\dot{\phi}$	Angular velocity of stance leg
γ	Angle of an inclined plane with horizontal
m_{H}	Mass of the hip
m	The lumped mass of each leg
l_{g2}	Length from the hip to the center of leg mass
l	Length of each leg
I	Inertial moment of each leg
g	Acceleration of gravity
$\mathbf{R}$	Field of real numbers
$\dot{()}$	Time derivation

Thus the stance leg and the swing leg ideally exchange each other at the transition. The condition of the transition is geometrically expressed as follows:

$$\theta + \phi = 2\gamma. \tag{2}$$

At the transition, two assumptions are given:

A1) The swing leg and the stance leg exchange each other instantaneously;

A2) The collision of the biped robot with the inclined plane is inelastic and nonslip.

Under these assumptions, the angular moment of biped robot is kept during the collision [9]. It allows us to treat the collision by the relation of the pre-impact, and the post-impact angular velocities. The relation is described as follows:

$$\begin{bmatrix} \theta^+ \\ \phi^+ \\ \dot{\theta}^+ \\ \dot{\phi}^+ \end{bmatrix} = \begin{bmatrix} 0 & 1 & 0 & 0 \\ 1 & 0 & 0 & 0 \\ 0 & 0 & N_{11}(\theta,\phi) & N_{12}(\theta,\phi) \\ 0 & 0 & N_{21}(\theta,\phi) & N_{22}(\theta,\phi) \end{bmatrix} \begin{bmatrix} \theta^- \\ \phi^- \\ \dot{\theta}^- \\ \dot{\phi}^- \end{bmatrix}, \tag{3}$$

where superscripts $^+$ and $^-$ describe the state of post-impact and pre-impact respectively. $N_{ij}(\theta,\phi), i,j = 1,2$ are obtained by the conservation law of angular momentum.

In the transition, the energy dissipation also occurs. In a steady walking, the energy dissipation at the transition is equal to the energy gained by the decrease of gravitational potential energy.

3. Numerical simulations

3.1. Steady gaits

Numerical simulations are performed for the biped robot as shown in Fig. 1. The parameters are set as shown in Tab. 2. Limit cycles in Eqs. (1) and (3) are shown in Fig. 2. As in [2], there exist two steady gaits. We call the gait corresponding orbit α by gait S, and orbit β by gait U. The jumps A and B in the figure correspond to the state jumps by Eq. (3). The trajectory from A to B shows the trajectory of stance leg. After the jump B, the trajectory is transposed to the trajectory of swing leg. As mentioned in previous section, the energy cost to walk for a distance is same in both gaits. The characteristics of both gaits are shown in Tab. 3. Thus, the gait S walks slowly with a long stride.

Table 2: Setting of parameters.

m_{H}	0.7	m	0.15	g	9.8
l	1.0	l_{g2}	0.5	γ	-0.01
I	0.0017				

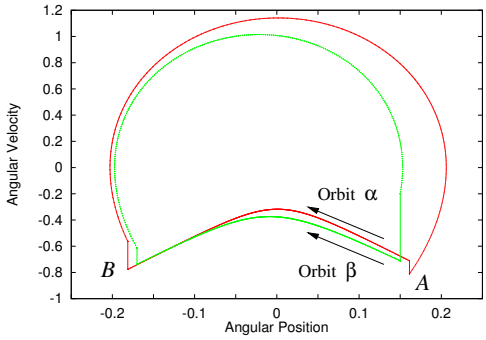

Figure 2: Limit cycles of passive dynamic walking. A and B indicate the state jump by Eq. (3).

Table 3: Physical characteristics of two gaits.

	stride	Period of Step	Average speed
Gait S	0.339	0.744	0.456
Gait U	0.319	0.652	0.487

3.2. Local stability of steady gaits

It is well known that there exists a stable steady gait in passive dynamic walking [3, 7, 8]. Let the state space $\boldsymbol{X}$ be a connected open subset of $\mathbf{R}^4$ and the state vector $\boldsymbol{x}$ be $\boldsymbol{x} = [\theta\ \phi\ \dot{\theta}\ \dot{\phi}]^{\mathrm{T}} \in \boldsymbol{X}$. $\boldsymbol{x}_k$ is now defined to be the value at the instance of post-transition on step k. The relation between the state of the next step $\boldsymbol{x}_{k+1}$ and $\boldsymbol{x}_k$ is then given:

$$\boldsymbol{x}_{k+1} = \boldsymbol{F}(\boldsymbol{x}_k), \tag{4}$$

where $\boldsymbol{F}$ denotes the nonlinear function called by step-to-step map [2]. In the neighborhood of fixed point at the instance of post-transition $\bar{\boldsymbol{x}}$, we can linearize the map as follows:

$$(\boldsymbol{x}_{k+1} - \bar{\boldsymbol{x}}) = \boldsymbol{D}(\boldsymbol{x}_k - \bar{\boldsymbol{x}}), \tag{5}$$

where $\boldsymbol{D}$ denotes linearized map in the neighborhood of $\bar{\boldsymbol{x}}$. The stability type of $\bar{\boldsymbol{x}}$ in Eq. (5) is determined by the magnitude of the eigenvalues of $\boldsymbol{D}$. The asymptotic behavior of Eq. (4) near $\bar{\boldsymbol{x}}$ and its stability type are also determined by the magnitude [10]. The fixed point of the orbit α is given as $\bar{\boldsymbol{x}}_\alpha = [0.161\ -0.181\ -0.711\ -0.563]^{\mathrm{T}}$, the point of the

orbit β $\bar{\boldsymbol{x}}_\beta = [0.150\ -0.170\ -0.712\ -0.613]^{\mathrm{T}}$. Eigenvalues of $\boldsymbol{D}$ are -0.50 ± 0.34i, -0.11, 0 at $\bar{\boldsymbol{x}} = \bar{\boldsymbol{x}}_\alpha$. The eigenvector of zero eigenvalue is correspond to the asymptotic line of Eq. (1) near $\bar{\boldsymbol{x}}$. Thus $\bar{\boldsymbol{x}}_\alpha$ is a stable fixed point and Gait S implies a stable gait. At $\bar{\boldsymbol{x}} = \bar{\boldsymbol{x}}_\beta$, eigenvalues are -2.11, -0.67, -0.05, 0. Therefore, $\bar{\boldsymbol{x}}_\beta$ is a hyperbolic saddle point, and U becomes an unstable gait.

3.3. The domain of attraction of stable gait

The domain of attraction of the biped robot is governed by the phase structure. Fig. 3 shows the domain of attraction of stable orbit α at post-transitional state. The figure denotes the sectional domain at $\theta^+ = 0.150$ which is equivalent to θ^+ of $\bar{\boldsymbol{x}}_\beta$. In this figure, $\bar{\boldsymbol{x}}_\beta$ lies on the boundary of the domain. Thus, the phase structure of the biped robot is transpired by the invariant manifold of $\bar{\boldsymbol{x}}_\beta$. Moreover the biped robot has constraint related to the ground. In this paper, the constraint is represented by $\{\dot{\theta} < -\dot{\phi} \mid \theta = \theta^+, \theta^-\}$. It implies that once the swing leg leaves from the ground, it is assumed to be controlled ideally. The control allows the biped robot to walk without stumbles.

Figure 4 shows the phase portrait of Eqs. (1) and (3) in the neighborhood of $\bar{\boldsymbol{x}}_\beta$. In the figure, $W^{\mathrm{u}}_{\mathrm{loc}}(\bar{\boldsymbol{x}}_\beta)$ denotes the local unstable manifold related to the maximum eigenvalue of $\boldsymbol{D}|_{\bar{\boldsymbol{x}}=\bar{\boldsymbol{x}}_\beta}$, and $W^{\mathrm{s}}_{-0.05}(\bar{\boldsymbol{x}}_\beta)$ the local stable manifold to the minimum eigenvalue of $\boldsymbol{D}|_{\bar{\boldsymbol{x}}=\bar{\boldsymbol{x}}_\beta}$ except zero eigenvalue. A blanch of local unstable manifold $W^{\mathrm{u}}_{\mathrm{loc}}(\bar{\boldsymbol{x}}_\beta)$ is converged to $\bar{\boldsymbol{x}}_\alpha$, and the local stable manifold $W^{\mathrm{s}}_{-0.05}(\bar{\boldsymbol{x}}_\beta)$ is truncated at C by the constraint of ground. In the figure, the trajectory from C to D is based on the constraint of ground, and $\dot{\theta}$ is equal to $-\dot{\phi}$ in the interval. Fig. 4(c) shows the phase structure on $\theta - \dot{\phi}/\dot{\theta}$ plane. The influence of the constraint is clearly observed in the figure. As in Eq. (3), the pre-impact state is linearly related to post-impact state. The phase structure is also discussed by Figs. 4(c) and (d). It implies that the biped robot continues walking when we set angular velocity of the swing leg $\dot{\phi}$ large, and the kinetic energy of the biped robot K low at small θ. At large θ, the domain of attraction becomes larger than the domain at small θ. Thus, any control of the biped robot is not required at large θ.

In Fig. 4, the local stable manifold $W^{\mathrm{s}}_{-0.05}(\bar{\boldsymbol{x}}_\beta)$ is truncated by the constraint of ground. Thus, the domain of at-

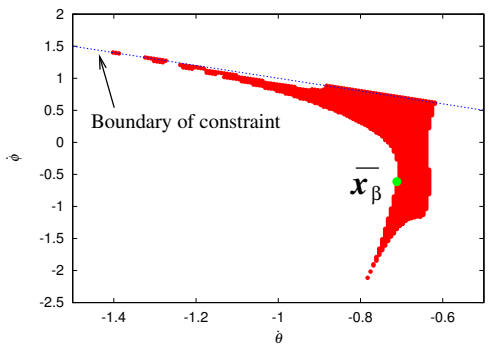

Figure 3: Sectional domain of attraction of the stable fixed point $\bar{\boldsymbol{x}}_\alpha(\theta^+ = 0.150)$.

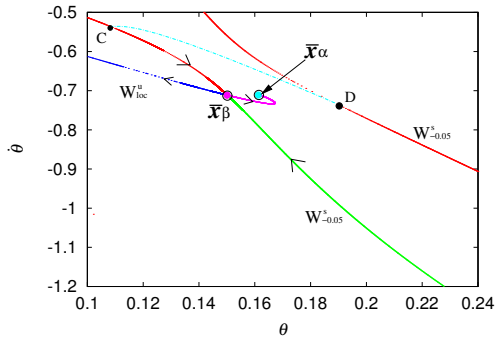

(a) θ–$\dot{\theta}$ plane

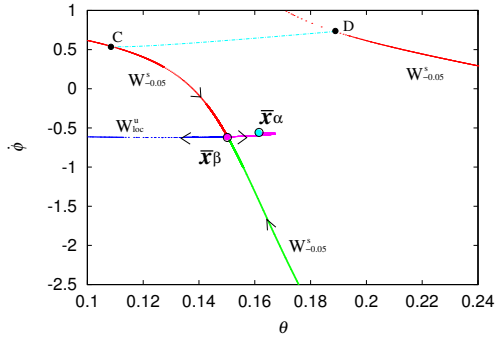

(b) θ–$\dot{\phi}$ plane

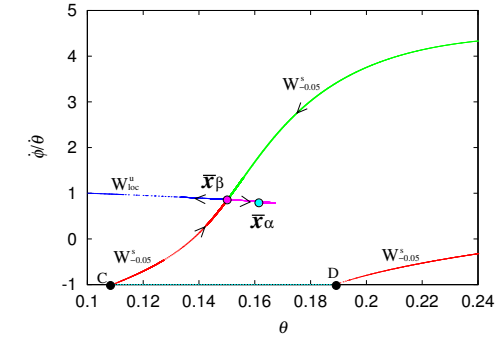

(c) θ–$\dot{\phi}/\dot{\theta}$ plane

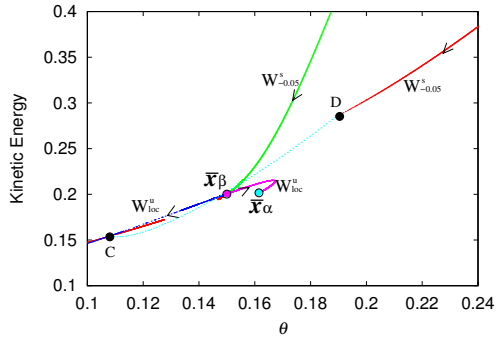

(d) θ–K plane

Figure 4: Sectional phase portraits in the neighborhood of $\bar{\boldsymbol{x}}_\beta$. Trajectory from C to D is based on the constraint of ground.

traction may be complex. However, it is out of the scope in this paper. Figs. 5 and 6 show some trajectory on $\theta-\dot{\theta}$ plane and $\theta-\dot{\phi}$. In the figures, each initial state $\boldsymbol{x}_i, i = 1, \cdots, 7$ belongs to the local manifolds $W^{\mathrm{s}}_{-0.05}(\bar{\boldsymbol{x}}_\beta)$ and $W^{\mathrm{u}}_{\mathrm{loc}}(\bar{\boldsymbol{x}}_\beta)$, or the hedge of the domain of attraction which is governed by the constraint. $E^s(\bar{\boldsymbol{x}}_\beta)$ is a stable subspace related to the eigenvalue of $\boldsymbol{D}|_{\bar{\boldsymbol{x}}=\bar{\boldsymbol{x}}_\beta}$. $\boldsymbol{x}_1$ corresponds to C in Fig. 4, and $\boldsymbol{x}_3$ to D in Fig. 4. $\boldsymbol{x}_2$ belongs to the hedge constraint of the ground. $\boldsymbol{x}_4, \boldsymbol{x}_5, \boldsymbol{x}_6$, and $\boldsymbol{x}_7$ are points on the local stable manifold $W^{\mathrm{s}}_{-0.05}(\bar{\boldsymbol{x}}_\beta)$. The behavior of each image of map is categorized into three types:

T1) The trajectories of $\boldsymbol{x}_1, \boldsymbol{x}_3, \boldsymbol{x}_4$, and $\boldsymbol{x}_7$ always belong to the domain of attraction shown in Fig. 4, and converge to the stable fixed point $\boldsymbol{x}_\alpha$;

T2) The trajectories of $\boldsymbol{x}_2$ and $\boldsymbol{x}_6$ converge to $\boldsymbol{x}_\alpha$, but escape from the domain during the transient;

T3) Though the initial condition $\boldsymbol{x}_5$ belongs to the domain, the trajectory will not converge.

The classification is explained by the stable subspace $E^s(\bar{\boldsymbol{x}}_\beta)$. The type T2) and T3) are divided on the subspace $E^s(\bar{\boldsymbol{x}}_\beta)$. The trajectories of $\boldsymbol{x}_2$ and $\boldsymbol{x}_6$ get out of the domain during the transients, but is always in the domain or inside of $E^s(\bar{\boldsymbol{x}}_\beta)$. The trajectory of $\boldsymbol{x}_5$ gets out of both the domain and $E^s(\bar{\boldsymbol{x}}_\beta)$. It implies that the stable manifold $W^{\mathrm{s}}_{-0.05}(\bar{\boldsymbol{x}}_\beta)$ mainly defines the flow of the Eqs. (1) and (3). The other subspace related to the eigenvalue of $\boldsymbol{D}|_{\bar{\boldsymbol{x}}=\bar{\boldsymbol{x}}_\beta}$ governs the global behavior.

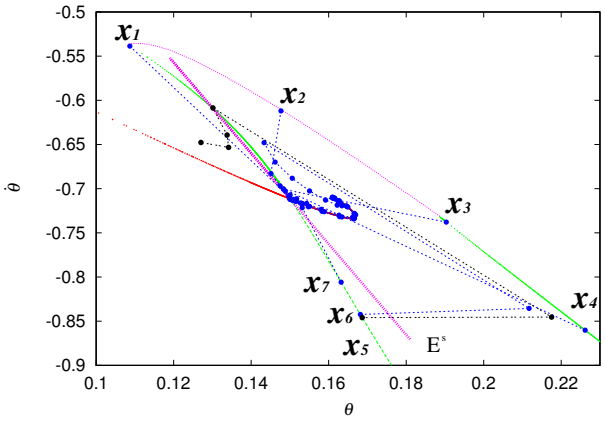

Figure 5: Trajectories on θ–$\dot{\theta}$ plane.

4. Remarks

In this paper, the stability of the simplest passive dynamic walking was numerically discussed. The mechanism of simple passive dynamic walking was schematically shown based on the phase structure, which is restricted by the constraint of the ground, and found to become complex in the neighborhood of unstable limit cycle.

The conditions to achieve the continuous walking and its phase structure give us a clue to design biped robots. It is our future project.

Acknowledgment

The authors would like to show their cordial appreciation to Dr. Yoshihiko Susuki for his fruitful discussions and comments.

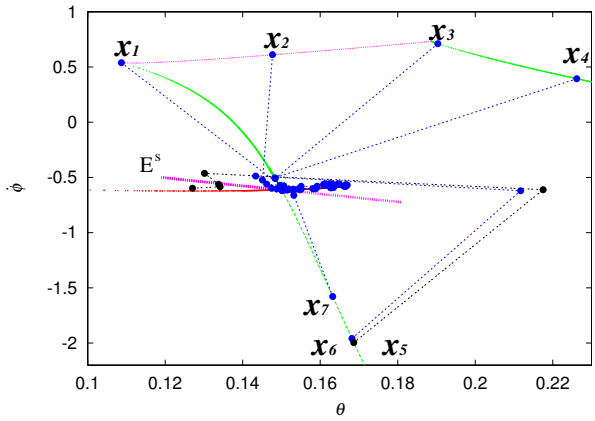

Figure 6: Trajectories on θ–$\dot{\phi}$ plane.

References

[1] T. McGeer, Passive Dynamic Walking, *Int. J. of Robotics Research*, **9**(2), 62–82 (1990).

[2] M. Garcia, A. Chatterjee and A. Ruina, M. Coleman, The simplest walking model: complexity, and scaling, *ASME J. of Biomechanical Engineering*, **120**(2), 281–288 (1998).

[3] A. Goswami, B. Espiau and A. Keramane, Limit cycle in a passive compass gait biped and passivity-mimicking control laws, *Autonomous Robots*, **4**(3), 273–286 (1997).

[4] K. Osuka and K. Kirihara, Motion Analysis and Experiment of Passive Walking Robot Quartet II, *Proc. of the 2000 IEEE Int. Conf. on Robotics and Automation*, 3052–3056 (2000).

[5] S. Collins, A. Ruina, R. Tedrake and M. Wisse, Efficient Bipedal Robots Based on Passive-Dynamic Walkers, *Science*, **307**, 1082–1085 (2005).

[6] Y. Sugimoto, K. Osuka, Walking Control of Quasi-Passive-Dynamic-Walking Robot Quartet III based on Delayed Feedback Control, *Proceeding of 5th International Conference on Climbing and Walking Robots*, France(2002).

[7] A. Goswami, B. Thuilot and B. Espiau, A study of the passive gait of a compass-like biped robot: symmetry and chaos, *International Journal of Robotics Research*, **17**(12), 1282–301 (1998).

[8] I. A. Hiskens, Stability of hybrid system limit cycles: application to the compass gait biped model, *Proceeding of the 40th IEEE Conference on Decision and Control*, 3052–3056 (2000).

[9] Y. Hurmuzlu and T. H. Chang, Rigid Body Collisions of a Special Class of Planar Kinematic Chains, *IEEE Transaction on System, Man, and Cybernetics*, **22**(5), 964–971 (1992).

[10] J. Guckenheimer and P. Holmes, *Nonlinear Oscillations, Dynamical Systems, and Bifurcations of Vector Fields*, Springer-Verlag, pp. 13–27(1990).